

ton, J. Tannis, A. Tilghman, J. D. Walecka, S. Wojcicki, and C. Zupancic for valuable assistance.

\*Supported by the National Science Foundation.

<sup>1</sup>L. L. Nemenov, *Sov. J. Nucl. Phys.* **16**, 67 (1973) [*Yad. Fiz.* **16**, 125 (1973)].

## Observation of Elastic Neutrino-Proton Scattering\*

D. Cline, A. Entenberg, W. Kozanecki, A. K. Mann, D. D. Reeder, C. Rubbia, J. Strait, L. Sulak, and H. H. Williams

*Department of Physics, Harvard University, Cambridge, Massachusetts 02138, and Department of Physics, University of Pennsylvania, Philadelphia, Pennsylvania 19174, and Department of Physics, University of Wisconsin, Madison, Wisconsin 53706*

(Received 13 April 1976)

We have observed thirty events of the process  $\nu p \rightarrow \nu p$  with a background expectation of seven events. The neutral-current to charged-current ratio  $\sigma(\nu p \rightarrow \nu p)/\sigma(\nu n \rightarrow \mu^- p)$  is measured to be  $0.17 \pm 0.05$  for  $0.3 < q^2 < 0.9$  (GeV/c)<sup>2</sup> where  $-q^2$  is the square of the four-momentum transfer to the proton.

Because of its simplicity, one of the most interesting weak neutral-current reactions is the elastic scattering of neutrinos by protons. Previous searches<sup>1</sup> for this reaction have been hampered by high neutron background, poor pion-proton separation, and/or low statistics. The addition of shielding does not necessarily eliminate the neutron-background problem because of the presence of  $\nu$ -induced neutrons in equilibrium with neutrinos. In this experiment the problem is significantly alleviated by using a detector of such large size that  $\nu$ -induced neutrons can be absorbed or detected through their interactions in the outer regions of the detector.

The experiment was performed at Brookhaven National Laboratory in a "wide-band" horn-focused neutrino beam. The target-detector [Fig. 1(a)] consists of twelve calorimeter modules containing a total of 33 tons of liquid scintillator.<sup>2</sup> Each module [Fig. 1(b)] is segmented into sixteen cells which are viewed at each end by phototubes. For an energy deposition greater than 3 MeV in a given cell, precise timing and the energy depositions are recorded for each tube. This information determines the position of the source of the energy deposition along the cylinder to  $\pm 10$  cm and its timing to  $\pm 0.5$  nsec.

The front half of the detector utilizes a close-packed geometry to be fully sensitive to neutrons and charged particles entering from the sides, top, and bottom. For example, a neutron passing through the detector would signal itself by colliding with protons in several, separated cells. The last half of the detector has four large drift chambers<sup>3</sup> interspersed among the calorimeters.

Each chamber contains two  $x$  planes and two  $y$  planes so that the angle as well as position of any tracks exiting from a module may be determined. We have measured a single-gap efficiency of 98% for particles with angles of up to  $60^\circ$  relative to the beam direction. The entire apparatus is housed in a blockhouse of 1.5-m-thick heavy concrete to shield against neutrons. A 2.4-m  $\times$  3.5-m liquid scintillation counter upstream of the first calorimeter is used to veto charged particles.

The calorimeters and drift chambers are continuously calibrated by accepting beam-associated muons along with neutrino-induced triggers; in addition, vertical cosmic-ray events, recorded between machine bursts, monitor the pulse height and timing of each phototube in the system.

To estimate the cosmic-ray background, the detector is activated between beam bursts for a period of time equal to the duration of the beam

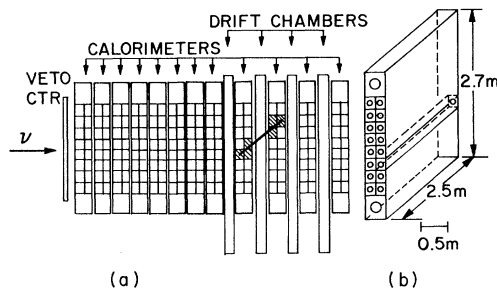


FIG. 1. (a) Side view of the apparatus showing a typical recoil proton event. (b) Diagram of a single calorimeter module.

spill. None of the events recorded during this gate satisfy the criteria imposed on neutrino-induced candidates.

The initial selection criterion for neutral-current events is containment, i.e., that neither the veto counter nor any cell in the farthest upstream calorimeter fires, and no energy deposition occurs within 40 cm horizontally or 46 cm vertically of the edge of any module nor in the most downstream 20 cm of the detector. From a data sample representing  $1.8 \times 10^{18}$  protons incident on the  $\nu$  target, events were selected which contained a single track that originated and stopped in the scintillator, and had an energy greater than 150 MeV.

The measured range, the pattern of energy depositions, and the total energy identify the particle. Since the range and energy loss for protons typically differ from that for pions by more than a factor of 2, the particle identification is relatively unambiguous. For example, shown in Fig. 2(a) is a plot of range versus energy for a sample of events selected as protons. A more quantitative discrimination is achieved by comparison of the calculated and observed energy deposition in each cell, an example of which is shown in the inset of Fig. 2(a). The results of fits to the proton and pion hypotheses are presented in Fig. 2(b). The  $\chi^2$  is on the average greater than the degrees of freedom because of the Landau distribution and calibration errors. A clear separation, however, occurs for all but 15% of the events which deposited  $\geq 150$  MeV of energy. Since we observe comparable numbers of proton and pion events, this ambiguity does not modify the total number of proton candidates.

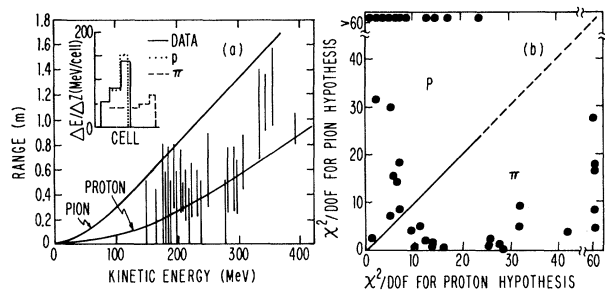


FIG. 2. (a) Plot of range versus energy for the selected  $p$  events (several events have been omitted for clarity). Each line indicates a measured range of the particle as determined by the number of cells that fire. Shown in the inset is the observed and calculated energy loss for a proton event. (b) Results of fits of the calculated to the observed energy depositions for proton and pion hypotheses.

Because of the rf structure of the proton beam, the neutrino beam consists of twelve bunches of 35-nsec duration (full width at half-maximum) occurring every 220 nsec. Figure 3(a) shows a plot of event time (modulo 220 nsec) for the selected proton events. The distribution is identical to that for  $\nu n \rightarrow \mu^- p$  events, except for a few events which occur later than 30 nsec (which are excluded from the final sample). We conclude that at most 1.5 of the in-time events could have been induced by slow neutrons originating far upstream.

We have included in this analysis only those events with energy  $T$  greater than 150 MeV. An inspection of all candidates suggests that those with  $T < 150$  MeV should be excluded for two reasons: (1) The proton-pion separation becomes increasingly ambiguous, and (2) nearly all triggers which occur outside the rf structure have  $T < 150$  MeV.

Additional evidence supporting the view that the proton candidates are neutrino induced is presented in Figs. 3(b) and 3(c), which display the vertex distributions for the proton events along the length of the detector and in the plane normal to the incident beam; within statistical error both distributions are uniform, showing no attenuation in the front or away from the edges. The distribution of angles of the recoil protons show

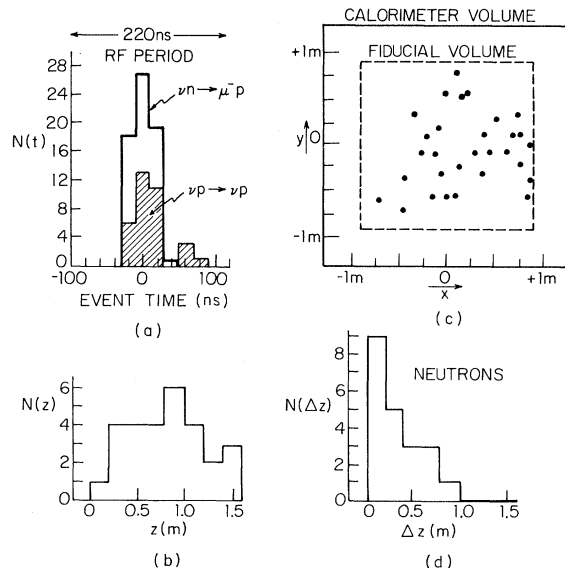


FIG. 3. (a) Distribution of event times for single protons (shaded) compared to that for a sample of charged-current elastic events. (b) Distribution of  $p$  vertices along the beam direction, and (c) in the plane normal to the beam direction. (d) Distribution of the distance between successive interactions for neutron events.

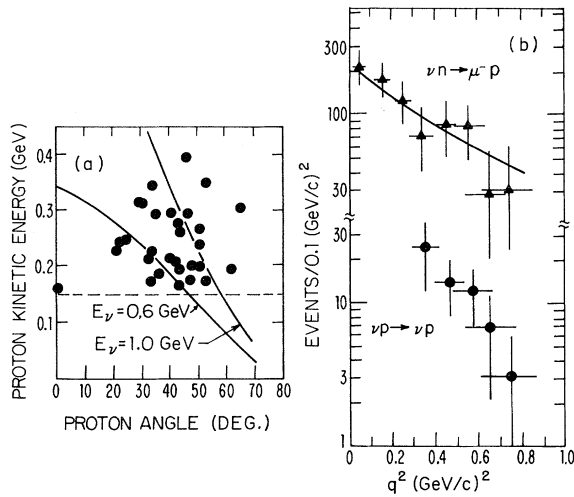


FIG. 4. (a) Kinetic energy versus angle for  $p$  events. The uncertainty in the energy is  $\pm 15\%$ . The absence of events below 150 MeV is due to the energy cut. Kinematic curves for  $\nu p \rightarrow \nu p$  are shown for two neutrino energies. (b) Observed, corrected,  $q^2$  distributions for  $\nu n \rightarrow \mu^- p$  and  $\nu p \rightarrow \nu p$ . The solid line is the calculated  $q^2$  distribution for  $m_A = 0.95 \text{ GeV}/c^2$ ,  $m_V = 0.84 \text{ GeV}/c^2$ . The horizontal error bars represent the uncertainty in the energy measurement.

no angular asymmetries, either up-down or left-right. In contrast, neutron-induced events, selected by requiring totally contained events with a second separate energy deposition, indicate a neutron interaction length of 40 cm [see Fig. 3(c)]. We conclude that the background from in-time neutrons, produced either far upstream or in nearby masses, is small.

Additional confirmation that the events arise from  $\nu$  elastic scattering is obtained from the angle-energy correlation of the protons. The neutrino flux is peaked at 1 GeV: Approximately 60% of the  $\nu n \rightarrow \mu^- p$  events observed correspond to  $\nu$  energies between 0.6 and 1.7 GeV. Shown in Fig. 4(a) is a plot of kinetic energy versus angle for the  $\nu p \rightarrow \nu p$  events. The majority of these events lie in the region expected for  $\nu p$  elastic scattering for incident neutrinos of this energy range. The energy distribution for  $\nu p \rightarrow \nu p$  events, when corrected for geometric acceptance, agrees with that for  $\nu n \rightarrow \mu^- p$  events. Protons from  $np \rightarrow np$  reactions induced by neutrons produced in nearby masses upstream would populate predominantly the region of the plot corresponding to  $E_\nu < 0.6 \text{ GeV}$ . From the  $T$ - $\theta$  distribution and the timing distribution, we estimate that a total of at most three of the events could be neutron induced.

Background from the  $\nu$ -induced reactions  $\nu n \rightarrow \nu \pi^- p$  and  $\nu n \rightarrow \mu^- p$  occurs if the second prong is contained in the vertex cell. From an extrapolation of the rate of two-prong events as the length of the second prong approaches the cell size, we estimate a background of at most two events. By a similar technique we estimate that the background from three- or more-prong events is negligible. The reaction  $\nu p \rightarrow \nu p \pi^0$  in which the  $\pi^0$  is not detected constitutes another source of background. The observed number of  $p \pi^0$  events<sup>4</sup> in the sample and the calculated  $\pi^0$  detection efficiency (75%) imply at most two events with an unseen  $\pi^0$ .

Charged currents of the type  $\nu n \rightarrow \mu^- p$  have been observed in the same sample as the  $\nu p \rightarrow \nu p$  events. For  $q^2 > 0.3 \text{ (GeV}/c^2)^2$ , the selection requirements for  $\nu n \rightarrow \mu^- p$  and  $\nu p \rightarrow \nu p$  are identical except for the presence of a muon; for  $q^2 < 0.3 \text{ (GeV}/c^2)^2$ ,  $\nu n \rightarrow \mu^- p$  candidates were primarily identified by their muon signature. The  $q^2$  distributions of the two samples of events, corrected for geometric acceptance<sup>5</sup> (calculated both analytically and by Monte Carlo techniques), are presented in Fig. 4(b). The observed shape of the  $q^2$  distribution for  $\nu n \rightarrow \mu^- p$  and the measured ratio of  $\nu n \rightarrow \mu^- p$  to the total cross section,  $0.25 \pm 0.03$ , are consistent with previous measurements.<sup>6</sup>

In conclusion, then, we have observed a total of thirty events that possess the required characteristics of neutrino-proton<sup>7</sup> elastic scattering; the background is estimated to be at most three events from  $np \rightarrow np$ , two events from  $\nu n \rightarrow \mu^- p$  and  $\nu n \rightarrow \nu \pi^- p$ , and two events from  $\nu p \rightarrow \nu p \pi^0$ . After subtraction, the number of  $\nu p \rightarrow \nu p$  events for  $0.3 < q^2 < 0.9 \text{ (GeV}/c^2)^2$ , when compared with the number of quasi-elastic events in the same  $q^2$  interval, yields a cross section ratio  $\sigma(\nu p \rightarrow \nu p)/\sigma(\nu n \rightarrow \mu^- p)$  of  $0.17 \pm 0.05$  where the error is statistical. This value is consistent with most of the broken-gauge-symmetry models involving the weak neutral current,<sup>8</sup> and with previous measurements.<sup>1</sup> A larger  $\nu$  sample and a  $\bar{\nu}$  exposure are currently being analyzed to provide a more quantitative test of the model.

We thank R. Rau, H. Foelsche, W. D. Walker, A. Pendzick, and the staff of the Brookhaven National Laboratory as well as the staffs of the High Energy Physics Laboratories at Harvard University, University of Pennsylvania, and University of Wisconsin for their immeasurable support during this work. A. Conners, D. DiBitonto, G. Gollin, J. Horstkotte, J. LoSecco, M. Merlin,

J. Rich, W. Smith, and M. Yudis aided in the set-up and initial running of the experiment.

\*Work supported in part by the U. S. Energy Research and Development Administration.

<sup>1</sup>D. C. Cundy *et al.*, Phys. Lett. **31B**, 478 (1970); P. Schreiner *et al.*, in *Proceedings of the Seventeenth International Conference on High Energy Physics, London, England, 1974*, edited by J. R. Smith (Rutherford High Energy Laboratory, Didcot, Berkshire, England, 1974), p. IV-123; C. Y. Pang *et al.*, unpublished.

<sup>2</sup>L. Sulak, in *Proceedings of the Calorimeter Workshop*, edited by M. Atac (Fermi National Accelerator Laboratory, Batavia, Ill., 1975), p. 155.

<sup>3</sup>D. C. Cheng *et al.*, Nucl. Instrum. Methods **117**, 157 (1974).

<sup>4</sup>If we assume that the number of  $\pi^+$  and  $\pi^-$  events are equal, the observed number of  $\pi^0/\pi^-$  neutral current events is consistent with the Gargamelle measurement on Freon. See G. H. Bertrand Cosemans *et al.*, Phys. Lett. **61B**, 207 (1976).

<sup>5</sup>The geometric acceptance for  $E_p = 1$  GeV and for tracks which go through at least one drift chamber is approximately 0.2, 0.45, and 0.33 for  $q^2 = 0.35, 0.55,$  and  $0.75$  (GeV/c)<sup>2</sup>, respectively.

<sup>6</sup>The value,  $0.25 \pm 0.03$ , that we determine for the ratio of the total quasielastic cross section to the total cross section, integrated over the Brookhaven National Laboratory neutrino energy distribution, is consistent with that obtained from data taken with the Brookhaven National Laboratory 7-ft bubble chamber: M. J. Murtagh, private communication; W. A. Mann *et al.*, Phys. Rev. Lett. **31**, 844 (1973).

<sup>7</sup>Events from the reaction  $\nu n \rightarrow \nu n$  would appear in our sample if  $np$  charge exchange occurs in the target nucleus or if it occurs after the neutron leaves the nucleus provided that the de-excitation of the target goes undetected (i.e.,  $< 3$  MeV of energy is deposited in the scintillator). We are currently evaluating the probability of these processes.

<sup>8</sup>S. Weinberg, Phys. Rev. D **5**, 1412 (1972); J. J. Sakurai and L. F. Urrutia, Phys. Rev. D **11**, 159 (1975); A. De Rújula, H. Georgi, and S. L. Glashow, Phys. Rev. D **12**, 3589 (1975); J. T. Gruenwald *et al.*, Bull. Am. Phys. Soc. **21**, 17 (1976); H. Fritzsche, M. Gell-Mann, and P. Minkowski, Phys. Lett. **59B**, 256 (1975); F. Wilczek, A. Zee, R. L. Kingsley, and S. B. Treiman, Phys. Rev. D **12**, 2768 (1975); M. Barnett, Phys. Rev. Lett. **34**, 41 (1975), and Phys. Rev. D **11**, 3246 (1975); S. Pakvasa, W. A. Simmons, and S. F. Tuan, Phys. Rev. Lett. **35**, 703 (1975).

### Observation in $e^+e^-$ Annihilation of a Narrow State at $1865 \text{ MeV}/c^2$ Decaying to $K\pi$ and $K\pi\pi\pi$ †

G. Goldhaber,\* F. M. Pierre,‡ G. S. Abrams, M. S. Alam, A. M. Boyarski, M. Breidenbach, W. C. Carithers, W. Chinowsky, S. C. Cooper, R. G. DeVoe, J. M. Dorfan, G. J. Feldman, C. E. Friedberg, D. Fryberger, G. Hanson, J. Jaros, A. D. Johnson, J. A. Kadyk, R. R. Larsen, D. Lüke,§ V. Lüth, H. L. Lynch, R. J. Madaras, C. C. Morehouse,|| H. K. Nguyen,\*\* J. M. Paterson, M. L. Perl, I. Peruzzi,†† M. Piccolo,‡‡ T. P. Pun, P. Rapidis, B. Richter, B. Sadoulet, R. H. Schindler, R. F. Schwitters, J. Siegrist, W. Tanenbaum, G. H. Trilling, F. Vannucci,‡‡ J. S. Whitaker, and J. E. Wiss

Lawrence Berkeley Laboratory and Department of Physics, University of California, Berkeley, California 94720, and Stanford Linear Accelerator Center, Stanford University, Stanford, California 94305

(Received 14 June 1975)

We present evidence, from a study of multihadronic final states produced in  $e^+e^-$  annihilation at center-of-mass energies between 3.90 and 4.60 GeV, for the production of a new neutral state with mass  $1865 \pm 15 \text{ MeV}/c^2$  and decay width less than  $40 \text{ MeV}/c^2$  that decays to  $K^+\pi^-$  and  $K^+\pi^-\pi^+\pi^-$ . The recoil-mass spectrum for this state suggests that it is produced only in association with systems of comparable or larger mass.

We have observed narrow peaks near  $1.87 \text{ GeV}/c^2$  in the invariant-mass spectra for neutral combinations of the charged particles  $K^+\pi^-$  ( $K\pi$ ) and  $K^+\pi^-\pi^+\pi^-$  ( $K3\pi$ ) produced in  $e^+e^-$  annihilation. The agreement in mass, width, and recoil-mass spectrum for these peaks strongly suggests they represent different decay modes of the same object. The mass of this state is  $1865 \pm 15 \text{ MeV}/c^2$

and its decay width (full width at half-maximum) is less than  $40 \text{ MeV}/c^2$  (90% confidence level). The state appears to be produced only in association with systems of comparable or higher mass.

Our results are based on studies of multihadronic events recorded by the Stanford Linear Accelerator Center-Lawrence Berkeley Laboratory magnetic detector operating at the colliding-beam